F$_1$-ATPase Changes Its Conformations upon Phosphate Release*

Tomoko Masaike‡§, Eiro Muneyuki‡, Hiroyuki Noji¶, Kazuhiko Kinosita, Jr.‡‡,
and Masasuke Yoshida‡ ‡‡§§¶¶**

*From the ‡Chemical Resources Laboratory, Tokyo Institute of Technology, 4259 Nagatsuta, Yokohama, 226-8503, Japan,
¶PRESTO (Precursory Research for Embryonic Science and Technology), Japan Science and Technology Corporation
332-0012, Japan, the ‖Institute of Industrial Science, University of Tokyo, 4-6-1 Komaba Meguro-ku, Tokyo 153-8505,
Japan, the **Center for Integrative Bioscience, Okazaki National Research Institutes, 38 Aza Nishigonaka,
Myodaiji-Cho, Okazaki, Aichi, 444-8585, Japan, ‡‡CREST (Core Research for Evolutional Science and Technology)
Genetic Programming Team 13, Teikyo University Biotechnology Center 3F, 907 Nogawa, Miyamae-ku,
Kawasaki 216-0001, Japan, and §§ERATO (Exploratory Research for Advanced Technology),
Japan Science and Technology Corporation 332-0012, Japan*

Motor proteins, myosin, and kinesin have γ-phosphate sensors in the switch II loop that play key roles in conformational changes that support motility. Here we report that a rotary motor, F$_1$-ATPase, also changes its conformations upon phosphate release. The tryptophan mutation was introduced into Arg-333 in the β subunit of F$_1$-ATPase from thermophilic *Bacillus* PS3 as a probe of conformational changes. This residue interacts with the switch II loop (residues 308–315) of the β subunit in a nucleotide-bound conformation. The addition of ATP to the mutant F$_1$ subcomplex α$_3$β(R333W)$_3$γδε caused transient increase and subsequent decay of the Trp fluorescence. The increase was caused by conformational changes on ATP binding. The rate of decay agreed well with that of phosphate release monitored by phosphate-binding protein assays. This is the first evidence that the β subunit changes its conformation upon phosphate release, which may share a common mechanism of exerting motility with other motor proteins.

ATP synthase is composed of the major subcomplexes F$_1$ and F$_o$. F$_1$-catalyzed synthesis of ATP from ADP and P$_i$ is coupled with proton translocation through F$_o$, which resides in the membrane. F$_1$ part can be separated from F$_o$ part as a water-soluble ATPase that has subunit composition α$_3$β$_3$γδε and hence is often called F$_1$-ATPase. Catalytic nucleotide-binding sites are located on the β subunits, whereas the α subunits contain noncatalytic nucleotide-binding sites. In the crystal structure of the bovine mitochondrial F$_1$-ATPase (MF$_1$),[1] the coiled-coil structure of the γ subunit is surrounded by a semi-hexagonal ring of α$_3$β$_3$ (1). F$_1$-ATPase is a rotary motor enzyme; ATP-dependent rotation of the γ subunit relative to the α$_3$β$_3$ ring, as predicted by biochemical studies (2–4), was visualized using the thermophilic F$_1$-ATPase (TF$_1$) (5). Consistent with the presence of three β subunits in the ring, hydrolysis of

a single ATP molecule drives a 120° rotation of the γ subunit (6). It is intriguing how the local conformational changes accompanied by each of reaction steps in the catalytic cycle, such as ATP binding, hydrolysis, and release of ADP and P$_i$, are amplified and transformed into the force to dislocate the γ subunit. Recent progress shows that each 120° rotation is further divided into a 90° substep that is driven by ATP binding and a 30° substep presumably driven by the release of the product, most likely ADP (7).

Nucleotide binding induces a large conformational change of the β subunit (8). Each of the three β subunits in the initial MF$_1$ structure, which was disclosed in 1994 (1), takes one of the two conformations: an "open" form in which catalytic site is empty or a "closed" form in which the catalytic site is occupied by AMP-PNP or ADP. Consistent with that, the β subunits of the crystal structure of the TF$_1$ subcomplex α$_3$β$_3$ without bound nucleotides were all in the open form (9). Compared with the open form, the carboxyl-terminal domain of the β subunit in the closed form swings ∼30° toward the amino-terminal domain so that the catalytic cleft located between two domains is closed. A nucleotide-induced transition from the open to the closed conformation is inherent in the nature of the β subunit, because even the isolated β subunit undergoes the open-close motion responding to nucleotide binding (10, 11). Thus, it has been proposed that the coordinated open-to-closed and closed-to-open motions of the β subunits in F$_1$-ATPase accompanied by ATP binding and ADP release drive 90° and 30° rotations of the γ subunit, respectively.

In contrast to the nucleotide-dependent open-close motion, the conformational events of the β subunit at the steps of hydrolysis of ATP and release of P$_i$ are unclear. In the case of other ATP-driven motor proteins, myosin and kinesin, the structures of the ATP-bound form and the ADP-bound form are different (12, 13), and P$_i$ release is assumed to be the step of power stroke (14, 15). The initial structure of MF$_1$, however, shows that the ADP-bound β subunit and the AMP-PNP-bound β subunit are in a very similar, closed conformation. Therefore, it appears that the loss of P$_i$ from the catalytic site does not cause significant conformational changes or that the intermediate species of the enzyme generated upon P$_i$ release is too unstable to form crystals even though its conformation is different from the known structures. Indeed, a third conformation of the β subunit was reported recently (16); one of the β subunits in the AlF$_4$⁻-inhibited MF$_1$ exists in a "half-closed" conformation, the catalytic site of which is occupied by ADP and sulfate in mimicry of P$_i$. Biochemical studies on the kinetics of P$_i$ release and the related conformational changes are few,

---

[1] The abbreviations used are: MF$_1$, bovine heart mitochondrial F$_1$; TF$_1$, thermophilic F$_1$-ATPase; AMP-PNP, adenosine 5′-(β,γ-imino) triphosphate; MDCC, [2-(1-maleimidyl)ethyl]-7-(diethylamino)-coumarin-3-carboxamide; PBP, phosphate-binding protein; ATPγS, adenosine 5′-O-(3-thiotriphosphate).

Conformational Changes of F$_1$-ATPase during Catalysis

mainly because of the absence of methods to monitor P$_i$ release from F$_1$-ATPase.

The present work has aimed at real time monitoring of conformational changes of the β subunit caused by P$_i$ release. Some Trp residues introduced into the β subunits of *Escherichia coli* F$_1$-ATPase were reported to confer different fluorescence between AMP-PNP binding and ADP binding (17–19). Fluorescently labeled γ subunit was also reported to change its conformations upon ATP cleavage (20, 21). Nevertheless, none of them reported fluorescence changes of the β subunit caused by P$_i$ release by time-resolved measurements. We have sought for new positions for the Trp mutation that can monitor changes of fluorescence upon P$_i$ release. Concurrently for that purpose, we have adopted the P$_i$-binding protein that enabled real time monitoring of P$_i$ release from the enzyme. Analyses, including kinetic comparison of fluorescence changes and P$_i$ release after addition of ATP, have established that a Trp introduced at position 333 (R333W) reflects P$_i$ release well. The residue 333 of the β subunit, located in helix H, which interacts with the "switch II loop," appears to sense γ-phosphate of the bound nucleotide and changes its conformation upon loss of P$_i$ from the catalytic site.

EXPERIMENTAL PROCEDURES

Reagents and Buffers—Nucleotides were purchased from Sigma and Roche Molecular Biochemicals. Mop reagents 7-methylguanosine and purine nucleotide phosphorylase were purchased from Sigma. The fluorescent probe for phosphate-binding protein, [2-(1-maleimidyl)ethyl]-7-(diethylamino)-coumarin-3-carboxamide (MDCC) was purchased from Molecular Probes. The buffers used in the measurements are abbreviated as follows: TK buffer, 50 mM Tris-HCl, pH 8.0, 100 mM KCl; TKM2 buffer, 50 mM Tris-HCl, pH 8.0, 100 mM KCl, 2 mM MgCl$_2$; TKM4 buffer, 50 mM Tris-HCl, pH 8.0, 100 mM KCl, 4 mM MgCl$_2$; KP$_i$ buffer, 100 mM KP$_i$, pH 7.0, 100 mM KCl, 2 mM EDTA; NaP$_i$ buffer, 100 mM NaP$_i$, pH 7.0, 200 mM NaCl; and reverse phase buffer: 100 mM NaP$_i$, pH 6.9, 4 mM EDTA. Unless otherwise indicated, TKM2 buffer was used for measurements. To eliminate contaminated P$_i$ from buffers, TKM and TK buffers for PBP assays contain 200 μM 7-methylguanosine and 0.01 unit/ml purine nucleotide phosphorylase (named P$_i$ mop) (22, 23).

Strains, Plasmids, and Preparation of Subcomplexes—*E. coli* strain JM109 was used for plasmid amplification. JM103Δ(*unc*B-*unc*D) was used for overexpression of the α, β, and γ subunits of F$_1$-ATPase. Plasmids used were pucβ, which carried a gene for the β subunit, for mutagenesis and expression, and pkk$\alpha\gamma$, which carried genes for the α and γ subunits, for expression. The βR333W and βD311W mutations into the β subunit were introduced by the Kunkel method (24) using primer oligonucleotides annealed to the single strand DNA of pucβ: 5′-GATAAATCCCCATCTCCGCAAGCTTCCACTCCAGGTTCGTC-3′ for βR333W introducing cleavage site of *Hind*III and 5′-CGTCGTGG-CCGGAGCCGGATCCGTATAGTCCCAGGCCGGGACGTAAATC-3′ for βD311W introducing cleavage site of *Bam*HI (mutated bases are underlined). For preparation of the isolated β(R333W) and $\alpha_3\beta$(D311W)$_3\gamma$, mutated plasmids were transformed into JM103Δ(*unc*B-*unc*D) for overexpression and purified using NaP$_i$ buffer as previously described (25). Because $\alpha_3\beta$(R333W)$_3\gamma$ and $\alpha_3\beta$(D311W/R333W)$_3\gamma$ could not be expressed using the pkk$\alpha\beta\gamma$ system, a novel lysate reassembly method was developed. The plasmids pkk$\alpha\gamma$, pucβ(R333W), and pucβ(D311W/R333W) were each expressed separately in JM103Δ(*unc*B-*unc*D). Pellets from centrifugation of the cultures were diluted in NaP$_i$ buffer. The cells containing mutated β subunits were each mixed with those containing the α and γ subunits. The mixture was disrupted by a French pressure cell and was incubated at 30 °C for 30 min for reassembly of the subcomplex. It was then incubated at 60 °C for 15 min, and the insoluble denatured proteins were removed by centrifugation for 40 min at 40,000 rpm. Purification of the subcomplexes were performed by ammonium sulfate gradient in NaP$_i$ buffer using a Butyl-Toyopearl 650M column (Tosoh). The purified β subunit and subcomplexes were stored as ammonium sulfate precipitates. They were diluted in TK buffer, concentrated by Vivaspin (Sartorius), and applied twice to a gel filtration (Superdex 200; Amersham Biosciences) for final purification (flow was 0.5 ml/min first with TK buffer and second with KP$_i$ buffer) on the day of measurements.

Analyses of Bound Nucleotides—Analysis of residual nucleotides after purification of the enzyme was performed as previously described

(26). The number of residual nucleotides bound to $\alpha_3\beta$(R333W)$_3\gamma$ was less than 0.1 mol/mol after gel filtration with KP$_i$ buffer and TK buffer.

The number of nucleotides bound to $\alpha_3\beta$(R333W)$_3\gamma$ at the end points of the fluorescence measurements was estimated by the following protocol. The mixtures of nucleotides and $\alpha_3\beta$(R333W)$_3\gamma$ from stopped flow measurements were each applied to an Ultrafree filtration device (molecular weight, 5 k cutoff; Millipore). After centrifugation for 2 min at 2 kilorounds per minute at 25 °C, the nucleotide contents in 100 μl of the filtrates were quantified by reverse phase high pressure liquid chromatography (ODS-80Ts; Tosoh) using reverse phase buffer. The amount of nucleotides bound to $\alpha_3\beta$(R333W)$_3\gamma$ was estimated by subtracting the concentration of the nucleotides free in solution (concentration in the filtrate) from the initial concentration.

Measurements of Trp Fluorescence—The fluorescence measurements of the Trp mutant subcomplexes and the isolated β(R333W) subunit were carried out by excitation at 295 nm, and detection of emission at 345 nm was carried out using a spectrofluorometer (FP-6500; Jasco). In a cuvette, 1.2 ml of 5 μM β(R333W) or 1 μM $\alpha_3\beta_3\gamma$ mutants was mixed with 20 μl of ATP or ADP while stirring.

Measurements of $\alpha_3\beta$(R333W)$_3\gamma$ were carried out also by a stopped flow apparatus (SFM-400; BioLogic) using a xenon lamp as a source of light. ATP in TK buffer (30 μl of 1.0 or 0.5 or 0.25 μM)[2] was mixed with the same volume of 2 μM $\alpha_3\beta$(R333W)$_3\gamma$ in TKM4 buffer over 20 ms. The same method was applied to ADP, AMP-PNP, and ADPγS. TK buffer prevents ATP at submicromolar concentrations from decomposition into ADP and P$_i$ before addition to $\alpha_3\beta$(R333W)$_3\gamma$. The same stopped flow experiments were also performed using buffers that were treated with P$_i$ mop to ensure that the buffer conditions were the same as those used for measurement of P$_i$ release. There was no change in the Trp fluorescence profile between with and without P$_i$ mop in solutions (data not shown).

Measurement of Unisite Catalysis—The unisite catalysis was measured using the stopped flow apparatus in the quenched flow mode. It was started by mixing 250 μl of 2 μM $\alpha_3\beta$(R333W)$_3\gamma$ with the same volume of 1 μM ATP and stopped after various time periods by perchloric acid quenching. Hydrolyzed nucleotides were analyzed by a reverse phase column (ODS-80Ts; Tosoh) using the reverse phase buffer as previously described (26).

Measurement of P$_i$ Release—Release of P$_i$ from $\alpha_3\beta$(R333W)$_3\gamma$ was measured using a PBP assay (22, 23). PBP labeled with MDCC was prepared as previously described (22, 23). Binding of P$_i$ to MDCC-labeled PBP (MDCC-PBP) increases the fluorescence emission at 464 nm when the complex is excited at 425 nm. By virtue of rapid binding of P$_i$ to MDCC-PBP ($k_{on} = 1.36 \times 10^8$ M^{-1} s^{-1}) and high affinity of PBP for P$_i$ ($K_d = \sim$0.1 μM) (22), the increase in the P$_i$ concentration in the solutions could be monitored as the increase of fluorescence emission in real time.

PBP assays were carried out using a stopped flow apparatus (SFM-400; BioLogic) under the same conditions as the Trp fluorescence measurements. 30 μl of 2 μM $\alpha_3\beta$(R333W)$_3\gamma$ in TKM4 buffer was mixed with the same volume of 4 μM MDCC-PBP and 1 μM ATP in TK buffer. The buffers contain P$_i$ mop for elimination of P$_i$ to avoid saturation of MDCC-PBP with contaminated P$_i$.

Measurement of the Rate of Formation of the MgADP-inhibited Form—To estimate the rate of formation of the MgADP-inhibited form under the fluorescence measurement conditions, the following experiment was carried out. 20 μl of 11 μM $\alpha_3\beta$(R333W)$_3\gamma$ and 200 μl of 0.55 μM ATP were manually mixed and preincubated at 25 °C for varying periods of time. 150 μl of the incubated solution was injected into the ATP-regenerating system (27) containing 2 mM ATP-Mg (mixture of equal concentrations of ATP and MgCl$_2$) in TKM2 buffer. The time course of ATP hydrolysis was measured by monitoring the absorbance at 340 nm using a spectrophotometer (V-550; Jasco). The slope of the absorbance is initially small as the majority of the molecules are in the MgADP-inhibited form, but it gradually increases because of reactivation by binding of ATP to the α subunit (28). Therefore, the ratio of active $\alpha_3\beta$(R333W)$_3\gamma$ was estimated from the initial slope of 10 s of absorbance at 340 nm compared with that without preincubation.

Other Assays—The concentrations of β(R333W), $\alpha_3\beta$(R333W)$_3\gamma$, $\alpha_3\beta$(D311W/R333W)$_3\gamma$, and $\alpha_3\beta$(D311W)$_3\gamma$ were analyzed by BCA assay (Pierce) and absorbance at 280 nm.

---

[2] All the stopped flow measurements and bound nucleotide measurements were repeated with 75 μl of mixing shots to be sure that the effects of carry-over from the previous shots were minimum. The rate constants and the amount of bound nucleotides (except for AMP-PNP, 0.41 mol/mol in Table I) were essentially the same ($\pm$ 5%) as those obtained with 30 μl/shot.
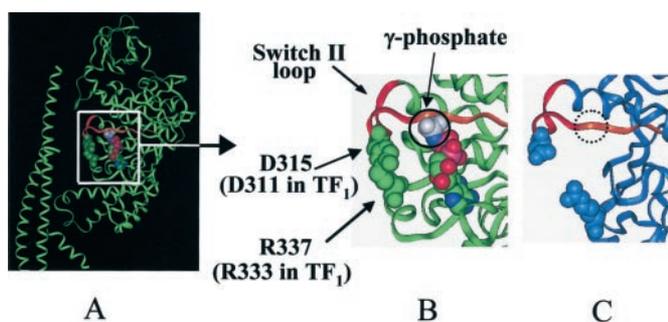
FIG. 1. **Positions of the residues Asp-315 and Arg-337 in bovine mitochondrial F₁ β subunit.** AMP-PNP and residues Asp-315 and Arg-337 are shown as space-filling models. The switch II loop is in *red*, and γ-phosphate of the bound nucleotide is in *white*. *A*, β subunit in the AMP-PNP bound form and the γ subunit. *B* and *C*, close-ups of the regions of Asp-315 and Arg-337 in AMP-PNP-bound β subunit (*B*) and nucleotide-free β subunit (*C*).

Data Processing—Data processing was performed by BioKine software (BioLogic), Origin 6.0 (Microcal Software), Excel 97 (Microsoft), and Dynafit (BioKin) (29).

RESULTS

Transient Increase in Trp Fluorescence upon ATP Binding— The initial crystal structure of MF₁ suggests that Arg-333 in TF₁-β (Arg-337 in MF₁-β) in helix H interacts with Asp-311 in TF₁-β (Asp-315 in MF₁-β) of the switch II loop only when the β subunit is in the closed conformation (Fig. 1) (1). Ren *et al.* (30) showed that cysteines introduced at positions 311 and 333 of TF₁-β can readily form an intramolecular cross-link in two of the three β subunits in the $\alpha_3\beta_3\gamma$ subcomplex of TF₁. Cross-linking abolished ATPase activity almost completely by fixing two β subunits in the closed conformation. We introduced Trps into the same positions and examined the fluorescence response of the mutant, expecting to have enabled fluorescent detection of nucleotide-induced open-close motion of the β subunits. Trp fluorescence of 1 μM $\alpha_3\beta$(D311W/R333W)$_3\gamma$ subcomplex decreased when 0.5 μM ADP was added (Fig. 2*A*). The fluorescent response to the same concentration of ATP was very different from that observed for ADP; a transient fluorescence increase was followed by rapid decay. The final level of fluorescence after decay was similar to that attained by ADP. Then, to determine which (or both) Trp was responsible for this transient fluorescence change, we made two single mutants, $\alpha_3\beta$(D311W)$_3\gamma$ and $\alpha_3\beta$(R333W)$_3\gamma$. The fluorescence response of $\alpha_3\beta$(D311W)$_3\gamma$ to ADP was similar to that of ATP, that is, a similar extent of increase and no further rapid changes (Fig. 2*B*). On the other hand, fluorescence of $\alpha_3\beta$(R333W)$_3\gamma$ showed a two-phase response to ATP addition: transient increase and rapid decay (Fig. 2*C*). The addition of ADP caused only a slight increase in fluorescence. The final level of fluorescence change by ATP was almost the same as that attained by ADP. It appeared that these two phases might represent certain steps in the catalysis occurring at a single catalytic site. Therefore, further fluorescence measurements were focused on $\alpha_3\beta$(R333W)$_3\gamma$, using a stopped flow apparatus, which could provide higher time resolution than manual mixing. It should be added that the three mutants mentioned above retained ATPase activity of rotary catalysis at a saturating ATP concentration (2 mM): 140 turnovers/s ($\alpha_3\beta$(D311W/R333W)$_3\gamma$), 29 turnovers/s ($\alpha_3\beta$(D311W)$_3\gamma$), and 106 turnovers/s ($\alpha_3\beta$(R333W)$_3\gamma$), which are 61, 13, and 46%, respectively, of that of the $\alpha_3\beta_3\gamma$ subcomplex without these mutations. Hereafter, we focus on the characteristics of $\alpha_3\beta$(R333W)$_3\gamma$.

Isolated β(R333W) Responds to ATP and ADP Different-ly—To understand whether the different fluorescence response
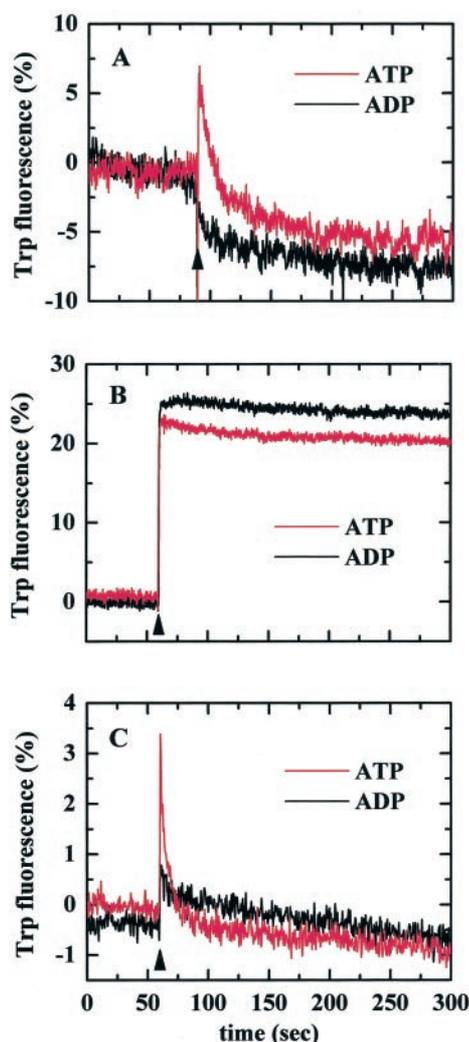

FIG. 2. **Time courses of fluorescence changes of the Trp mutants.** At the times indicated by *arrowheads*, ATP or ADP was manually mixed with $\alpha_3\beta$(D311W/R333W)$_3\gamma$ (*A*), $\alpha_3\beta$(D311W)$_3\gamma$ (*B*), and $\alpha_3\beta$(R333W)$_3\gamma$ (*C*). The concentrations of subcomplexes and nucleotides in the mixtures were 1 and 0.5 μM, respectively. The details of the experiments are described under "Experimental Procedures."

of $\alpha_3\beta$(R333W)$_3\gamma$ to ATP or ADP is generated from intersubunit interaction in the subcomplex or from conformational changes within a β subunit, fluorescence response of the isolated β(R333W) subunit to ATP or ADP was examined. Because the isolated β subunit can bind nucleotide but does not retain catalytic ability (31), the nucleotide-induced change of Trp fluorescence of β(R333W) can be solely attributed to the nucleotide binding. The addition of ATP or ADP to the isolated β(R333W) caused an instantaneous increase in Trp fluorescence that was followed by a slow increase (~30 s), and the fluorescence remained constant after saturation (Fig. 3*A*). The reason for the slow increase is not known, but it is worth noting that the extent of the fluorescence increase by ATP is significantly larger than by ADP, just as observed for initial fluorescence increase of $\alpha_3\beta$(R333W)$_3\gamma$. The K_d values for ATP and ADP estimated from fluorescence changes at various concentrations of nucleotide (Fig. 3*B*) are similar to each other: 20 μM for ATP and 27 μM for ADP, consistent with the values reported previously (32). These results suggest that conformational changes within a β subunit induced by AT(D)P binding can explain the initial increase of fluorescence observed for the $\alpha_3\beta$(R333W)$_3\gamma$ subcomplex. The different magnitude of fluorescence increase in response to ATP and ADP indicates that the

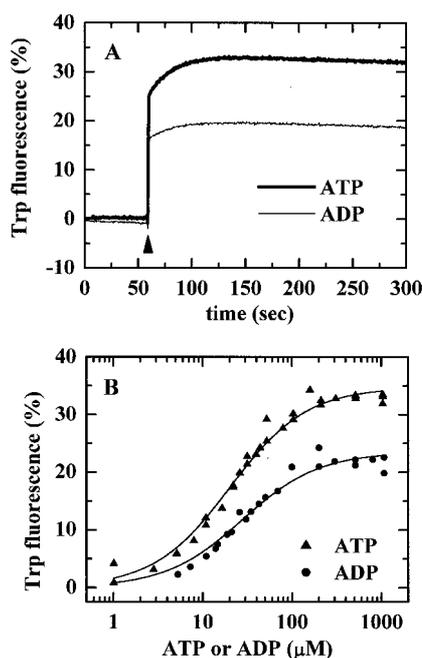FIG. 3. **Trp fluorescence changes of the isolated β(R333W) subunit induced by binding of ATP and ADP.** *A*, time course of Trp fluorescence changes induced by manual mixing with ATP or ADP at the time indicated by an *arrowhead*. Final concentrations of the β(R333W) subunit and nucleotides were 5 μM and 1 mM, respectively. *B*, the extent of Trp fluorescence changes of the isolated β(R333W) subunit (final concentration, 5 μM) induced by manual mixing with various concentrations of ATP or ADP. The *lines* indicate fits for calculations of the dissociation constant (K_d) by the following equation: $y = C \cdot [1 + x + K_d - sqrt \{(1 + x + K_d)^2 - 4x\}]/2$. The details of the experiments are described under "Experimental Procedures."

Trp residue introduced at position 333 of the β subunit is able to sense the presence of γ-phosphate of the bound adenine nucleotides, and this ability is inherent in the β(R333W) subunit.

Initial Fluorescence Increase Reflects ATP Binding—For $\alpha_3\beta$(R333W)$_3\gamma$, the initial increase in fluorescence by the addition of ATP was our initial focus (Fig. 4). The addition of a nonhydrolyzable ATP analog, AMP-PNP, to $\alpha_3\beta$(R333W)$_3\gamma$ induced an increase in fluorescence that was similar to that observed for ATP, but no subsequent decay was observed (Fig. 4*A*). Similarly, the decay was not observed for binding of ATP in the absence of Mg, where hydrolysis was blocked (data not shown). Another ATP analog, ATPγS, which is a poor substrate for F₁, also induced a similar fluorescence increase (Fig. 4*A*) that was followed by a slower decay. Taken together, we concluded that the initial fluorescence increase reflected the occupation of a catalytic site of the β subunit by ATP (*step 1* of Scheme 1). The rates of nucleotide binding calculated from the fluorescence changes of $\alpha_3\beta$(R333W)$_3\gamma$ were $(1.7 \pm 0.3) \times 10^7$ M^{-1} s^{-1} for ATP, $(4.1 \pm 0.7) \times 10^7$ M^{-1} s^{-1} for ADP, $(1.3 \pm 0.0) \times 10^6$ M^{-1} s^{-1} for AMP-PNP, and $(2.8 \pm 0.2) \times 10^7$ M^{-1} s^{-1} for ATPγS.

Nucleotide Binding Is Not the Cause of Fluorescence Decay— Decay of the fluorescence of $\alpha_3\beta$(R333W)$_3\gamma$ after the initial increase was observed under the conditions where unisite catalysis (33–35) was occurring and hence may correspond to a certain step of catalysis after the capture of ATP by a catalytic site. 0.5, 0.25, and 0.125 μM ATP caused the decay at comparable rates,[3] which indicates that the binding step is not involved in the decay (time courses are not shown). From the time

---

[3] The rates of decay estimated by the simple fitting scheme F₁ + ATP → F₁·ATP → F₁·ADP + P$_i$ attributing fluorescence increase to binding of ATP and decay to hydrolysis were k_{decay} = 1.9 ± 0.3, 1.8, and 2.0 s^{-1} for 0.5, 0.25, and 0.125 μM ATP, respectively.
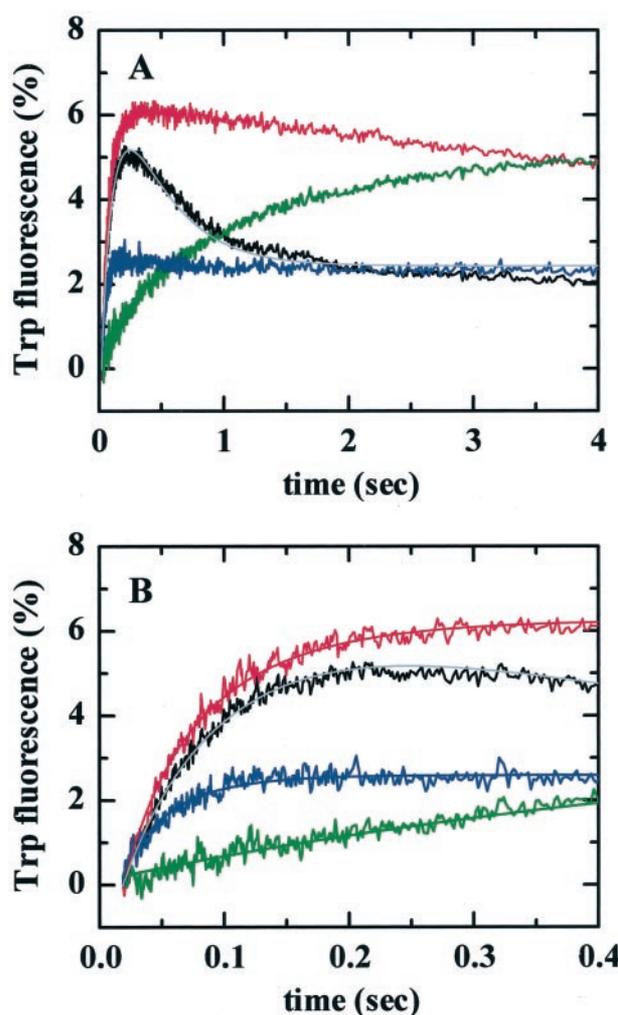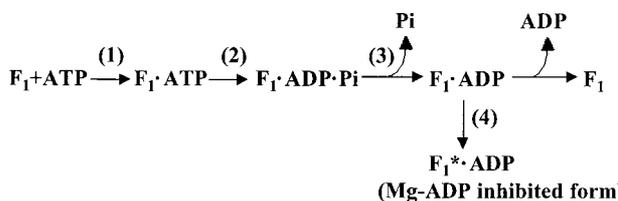

FIG. 4. **Time courses of Trp fluorescence changes of $\alpha_3\beta$(R333W)$_3\gamma$ induced by mixing with various nucleotides using a stopped flow apparatus.** Final concentrations of $\alpha_3\beta$(R333W)$_3\gamma$ and nucleotides were 1 and 0.5 μM, respectively. ATP is in *black*, ADP is in *blue*, AMP-PNP is in *green*, and ATPγS is in *red*. The base line is subtracted from each trace. The changes from the start of the measurements (18.6 ms) are plotted. *A*, changes in 4 s. A *line* overlaid with the *trace* of ATP is a simulation curve according to the following scheme: F₁ + ATP → F₁·ATP → F₁·ADP·P$_i$ → F₁·ADP + P$_i$. The rate constants used for the simulation are k_{on} = 1.4×10⁷, k_{cat} = 14.2, and k_{off} = 2.73, assuming that the increase in Trp fluorescence occurs by binding of ATP and that the decay occurs by release of P$_i$ from F₁. These rate constants are within the standard error of those derived from measurements of ATP hydrolysis and P$_i$ release in the following sections (see also Figs. 5 and 6 and Table I). *B*, changes in 0.4 s. The *lines* indicate fitting curves for calculating the binding rates (k_{on}) by the following scheme: F₁ + nucleotide → F₁·nucleotide. In the case of ATP, the same fitting curve as *A* is shown. The details of the experiments are described under "Experimental Procedures."

SCHEME 1. **Reaction scheme of uni-site ATP hydrolysis by F₁ ATPase.**

courses of Trp fluorescence upon the addition of various nucleotides (Fig. 4*A*), it is assumed that ATP hydrolysis or an event that occurs immediately after that causes fluorescence decay.
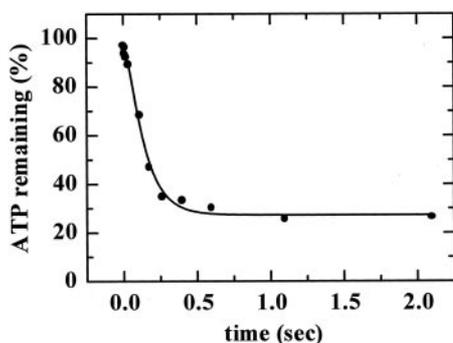
FIG. 5. **Time course of ATP hydrolysis by $\alpha_3\beta(R333W)_3\gamma$ under unisite conditions.** The reactions were performed by the quenched flow mode of stopped flow apparatus. Concentrations of $\alpha_3\beta(R333W)_3\gamma$ and nucleotides in the mixture were 1 and 0.5 μM, respectively. The reactions were stopped by the addition of perchloric acid, and the amounts of ATP and ADP were measured. The *line* is a fitting curve according to the following scheme: $F_1 + ATP \rightarrow F_1 \cdot ATP \rightarrow F_1 \cdot ADP \cdot P_i$ using $k_{on} = 1.7 \times 10^7$. The details of the experiments are described under "Experimental Procedures."

Typically, a slowly hydrolyzed ATP analog, ATPγS, causes slow decay.

ATP Hydrolysis Precedes Fluorescence Decay—To test the assumption described above, the time course of generation of ADP (*step 2* of Scheme 1) was measured. $\alpha_3\beta(R333W)_3\gamma$ and ATP were mixed using a stopped flow apparatus under the same conditions as the fluorescence measurements, and the reactions were stopped after various periods of time by the addition of perchloric acid. Acid quenching liberates substrates from denatured enzymes. Therefore, irrespective of whether the substrate is released or still bound to the enzyme, the generation of ADP can be detected by this method. The generation of ADP occurred with the rate constant of 14.4 s^{-1} (Fig. 5), which is greater than the rate of fluorescence decay (2.7 s^{-1}; Fig. 4). Therefore, the cause of fluorescence decay can be assigned to a step after ATP hydrolysis such as P$_i$ release and/or ADP release, etc. To determine which is the case, the release of ADP and P$_i$ was examined.

ADP Remains Bound after Hydrolysis—Analysis of the enzyme-bound nucleotides was carried out by sampling the mixtures of 1 μM $\alpha_3\beta(R333W)_3\gamma$ and 0.5 μM nucleotides from stopped flow fluorescence measurements and applying them each to an Ultrafree filtration device. The amount of nucleotides in the filtrates was analyzed. Virtually all (92%) of the product ADP remained bound to the enzyme even after all of the ATP had been hydrolyzed (Table I). Therefore, it is not feasible to assign the fluorescence decay to ADP release as the cause of the fluorescence decrease. We also measured the amount of enzyme-bound nucleotide when ADP, AMP-PNP, and ATPγS were added. Again, nearly all of the added nucleotides were stably bound to the enzyme (Table I). Taking this into account, the highest Trp fluorescence level by ATP, ATPγS, and AMP-PNP (Fig. 4A) can be assigned to the γ-phosphate (γ-thiophosphate)-bound form.

P$_i$ Release Proceeds at the Same Rate as Fluorescence Decay—To monitor the time course of P$_i$ release from the enzyme (*step 3* of Scheme 1), a PBP assay was adopted. Fluorescence of a coumarin-labeled PBP (MDCC-PBP) increases severalfold when P$_i$ binds. The versatility of monitoring of P$_i$ release from $\alpha_3\beta(R333W)_3\gamma$ by the PBP assay was carefully assessed and established (see "Experimental Procedures"). Thus, real time, continuous monitoring of P$_i$ released from F$_1$-ATPase became possible for the first time. We found that P$_i$ was released from $\alpha_3\beta(R333W)_3\gamma$ with a rate constant of 2.8 $\pm$ 0.1 s^{-1} (Fig. 6), which is the same rate as that of the fluorescence decay (Fig. 4). Thus, it is suggested that the decay of fluorescence after the initial increase reflects the decay of the enzyme form with

TABLE I
Concentrations of nucleotides remained bound to 1 μM of $\alpha_3\beta(R333W)_3\gamma$ after incubation with 0.5 μM of nucleotides

The samples were the same as those used for fluorescence observation using a stopped flow apparatus. ATP and ATPγS were detected as ADP because of hydrolysis by $\alpha_3\beta(R333W)_3\gamma$. The details of the experiments are described under "Experimental Procedures."

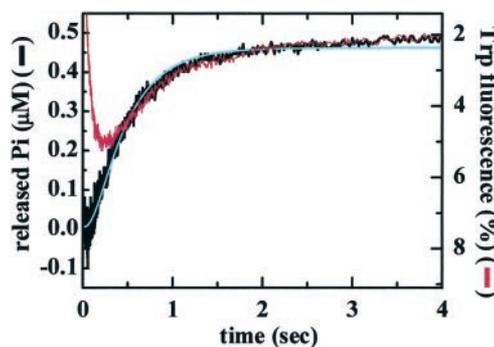| Nucleotide	Bound concentration
	μM
ATP	0.46
ADP	0.45
AMP-PNP	0.46
ATPγS	0.45

FIG. 6. **Time course of P$_i$ release from $\alpha_3\beta(R333W)_3\gamma$ monitored by fluorescence increase of MDCC-PBP.** ATP was mixed with $\alpha_3\beta(R333W)_3\gamma$ using a stopped flow apparatus. The final concentrations of $\alpha_3\beta(R333W)_3\gamma$ and nucleotides were 1 and 0.5 μM, respectively. The saturated level of MDCC-PBP fluorescence is set 0.5 μM. For comparison, the profile of Trp fluorescence changes under the same conditions is superimposed (*red*). A *blue line* indicates the fit of the MDCC-PBP fluorescence by the following scheme: $F_1 + ATP \rightarrow F_1 \cdot ATP \rightarrow F_1 \cdot ADP \cdot P_i \rightarrow F_1 \cdot ADP + P_i$ using $k_{on} = 1.7 \times 10^7$ and $k_{cat} = 14.4$. The details of the experiments are described under "Experimental Procedures."

bound ADP-P$_i$ to the enzyme form with bound ADP only, that is, release of P$_i$ from the enzyme. However, if there is a rapid conversion from the active enzyme-ADP complex into inactive enzyme-ADP complex, this conversion is also a candidate for the fluorescence decay. This possibility should be considered because it is known that the so-called MgADP-inhibited form, an inactive form of enzyme-ADP complex, tends to be generated under these conditions. We examined this possibility next.

Transition to the MgADP-inhibited Form Is Slower than Fluorescence Decay—The MgADP-inhibited form (*step 4* of Scheme 1) is not caused by a mere product inhibition but by stable retention of MgADP at the catalytic site. The MgADP can either be picked up from the bulk phase medium or can be a remnant of hydrolysis that remains bound to the enzyme (27). When the MgADP-inhibited form of F$_1$-ATPase is exposed to ATP and Mg^{2+}, it shows no ATPase activity initially but is gradually reactivated with a time constant of ~30 s (27, 43). Therefore, the population of the MgADP-inhibited form in a certain preparation of F$_1$-ATPase can be assessed from the initial rate of ATP hydrolysis. Under the same conditions used for the fluorescence measurement, we took an aliquot from the solution at the indicated times, injected it into the ATPase assay mixture and measured the initial ATPase activity. The initial ATPase activities were plotted as a function of the time and the rate of generation of the MgADP-inhibited form in the solution was estimated (Fig. 7). The time constant of the onset of MgADP inhibition thus estimated was 15 s, which is much slower than the fluorescence decay. Therefore, the possibility that the fluorescence decay is caused by generation of the MgADP-inhibited state is unlikely. In other words, the lifetime of active MgADP bound form is long enough to be maintained during fluorescence changes of several seconds. Taking these
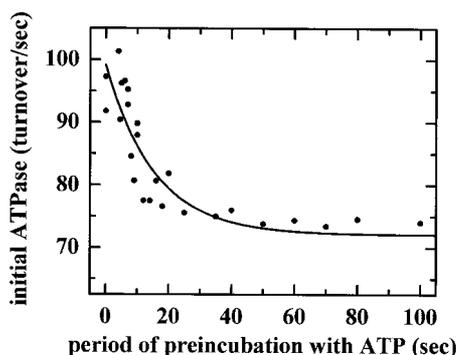
Fig. 7. **Formation of the MgADP-inhibited form under the unisite conditions.** $\alpha_3\beta$(R333W)$_3\gamma$ (1 μM) was preincubated with 0.5 μM ATP. An aliquot of the mixture was taken out after the indicated preincubation period and injected into the ATPase assay mixture, and an initial velocity of ATP hydrolysis was measured that reflected the proportion of the active form and the MgADP-inhibited form of the subcomplex generated during preincubation with ATP. The details of the experiments are described under "Experimental Procedures."

TABLE II
Rate constants of the reaction steps and corresponding Trp fluorescence changes

Reaction step	Step in Scheme 1	Rate constant	Trp fluorescence
ATP binding	1	$(1.7 \pm 0.3) \times 10^7 \mathrm{M}^{-1}\mathrm{s}^{-1}$	Increase
ATP hydrolysis	2	$14.4 \pm 0.2 \mathrm{\,s}^{-1}$	Negligible change
P$_i$ release	3	$2.8 \pm 0.1 \mathrm{\,s}^{-1}$	Decay
ADP inhibition	4	$6.7 \times 10^{-2} \mathrm{\,s}^{-1}$	

results together, we can conclude that under unisite conditions, the increase in Trp fluorescence of the $\alpha_3\beta$(R333W)$_3\gamma$ subcomplex occurs upon ATP binding, and the decay occurs as a function of P$_i$ release (Table II).

DISCUSSION

The novel Trp mutant $\alpha_3\beta$(R333W)$_3\gamma$ revealed that the residue Arg-333 senses the presence of γ-phosphate at the catalytic site of β subunit as well as changes in the surrounding structure upon nucleotide binding and P$_i$ release. Although Arg-333 does not directly contact the γ-phosphate of the bound nucleotide in the crystal structure, this residue somehow recognizes conformational differences between ATP-bound (or ADP-P$_i$-bound) and ADP-bound conformations of the β subunit.

It is worth noting that when a nucleotide is bound to the catalytic site, the mutated residue Arg-333 interacts with the switch II loop, a switch region common to a wide range of nucleotide triphosphate-utilizing proteins including GTP-binding proteins and motor proteins (12, 13, 36–40). A function of switch II in myosin and kinesin is to transmit conformational changes caused by γ-phosphate release to a distant point where motility of motor proteins is exerted (41). For example, in the case of myosin, an alanine mutation introduced into Gly-457 in the switch II loop causes loss of motility (42). In the crystal structure of monomeric kinesin motor KIF1A, the switch II loops of the ADP-bound and ATP-bound forms were in different conformations (12). Moreover, studies using fluorescence energy transfer and other analyses of conventional kinesin indicated a difference between ATP-bound and ADP-bound forms in the flexibility of the neck linker (15). Therefore, it is natural to assume that F$_1$-ATPase, another motor protein, might undergo an analogous conformational change when P$_i$ is released.

However, real images of the conformational change of F$_1$-ATPase that we detected by the fluorescence change cannot be directly assumed by comparing crystal structures of various nucleotide binding states that are solved to date. The crystal structure of F$_1$-ATPase containing β subunits in the ATP-bound, ADP-bound, and empty forms in one molecule (1) suggested that P$_i$ release does not cause drastic conformational changes because the structure of AMPPNP-bound and ADP-bound β subunits are very similar to each other, both in the same closed conformation. There is a possibility that introduced Trp reflects a very subtle change in the conformation accompanying P$_i$ release. A new crystal structure (16) was discovered recently that contains a third half-closed conformation of the β subunit, which is in between the closed and open

forms. This new conformation is thought to be in a transition state where the products ADP and P$_i$ are both bound. The existence of this half-closed conformation indicated partial opening of the β subunit during ATP hydrolysis. As a next step, further opening of ADP-bound form induced by P$_i$ release can naturally be assumed. Therefore, another possibility is that the fluorescence change reflects the difference of these two partially open states: one with bound ADP-P$_i$ and the other with bound ADP. This problem has direct implications on the conformational transitions accompanying the catalytic cycle but awaits further studies to be clarified.

The present research also revealed new information about the ATPase reaction by direct, real time measurements of some of the kinetic parameters of the unisite catalysis (Table II). The parameters shown here give insights into the reaction mechanism. The first is the rate of nucleotide binding. Comparing the results of stopped flow measurements (unisite catalysis conditions) with the previous single molecule observation of rotating F$_1$-ATPase at low ATP concentrations (bi-site or tri-site catalysis conditions), the rates of ATP binding are in the same range ($(1.7 \pm 0.3) \times 10^7 \mathrm{M}^{-1} \mathrm{s}^{-1}$ and $2.7 \times 10^7 \mathrm{M}^{-1} \mathrm{s}^{-1}$, respectively). This indicates that the rates of ATP binding are almost the same for the first and second (or third) catalytic sites. The second is that P$_i$ release predominantly occurs while ADP remains bound to the enzyme in unisite catalysis. The third is that the rate of P$_i$ release is slower than that of ATP hydrolysis, suggesting that the F$_1$·ADP·P$_i$ complex has to wait for some conformational change that allows P$_i$ release.

Future studies should be directed at the observation of conformational changes of the β subunit in F$_1$-ATPase at each step (including P$_i$ release) of during rotational catalysis. For this purpose, a new probe that is tractable by single molecule observation is necessary.

REFERENCES

1. Abrahams, J. P., Leslie, A. G. W., Lutter, R., and Walker, J. E. (1994) *Nature* **370,** 621–628
2. Boyer, P. D. (1993) *Biochim. Biophys. Acta* **1140,** 215–250
3. Boyer, P. D., and Kohlbrenner, W. E. (1981) in *Energy Coupling in Photosynthesis*, pp. 407–426, Elsevier Science Publishing Co., Inc., New York
4. Duncan, T. M., Bulygin, V. V., Zhou, Y., Hutcheon, M. L., and Cross, R. L. (1995) *Proc. Natl. Acad. Sci. U. S. A.* **92,** 10964–10968
5. Noji, H., Yasuda, R., Yoshida, M., and Kinosita, K., Jr. (1997) *Nature* **386,** 299–302
6. Yasuda, R., Noji, H., Kinosita, K., Jr., and Yoshida, M. (1998) *Cell* **93**, 1117–1124
7. Yasuda, R., Noji, H., Yoshida, M., Kinosita, K. Jr., and Ito, H. (2001) *Nature* **410**, 898–904
8. Tsunoda, S. P., Muneyuki, E., Amano, T., Yoshida, M., and Noji, H. (1999) *J. Biol. Chem.* **274,** 5701–5706
9. Shirakihara, Y., Leslie, A. G. W., Abrahams, J. P., Walker, J. E., Ueda, T., Sekimoto, Y., Kambara, M., Saika, K., Kagawa, Y., and Yoshida, M. (1997) *Structure* **5,** 825–836
10. Tozawa, K., Sekino, N., Soga, M., Yagi, H., Yoshida, M., and Akutsu, H. (1995) *FEBS Lett.* **376,** 190–194
11. Yagi, H., Tozawa, K., Sekino, N., Iwabuchi, T., Yoshida, M., and Akutsu, H. (1999) *Biophys. J.* **77,** 2175–2183
12. Kikkawa, M., Sablin, E. P., Okada, Y., Yajima, H., Fletterick, R. J., and

Hirokawa, N. (2001) *Nature* **411,** 439–445
13. Houdusse, A., Kalabokis, V. N., Himmel, D., Szent-Gyorgyi, A. G., and Cohen C. (1999) *Cell* **97,** 459–470
14. Suzuki, Y., Yasunaga, T., Ohkura, R., Wakabayashi, T., and Sutoh, K. (1998) *Nature* **396,** 380–383
15. Rice, S., Lin, A. W., Safer, D., Hart, C. L., Naber, N., Carragher, B. O., Cain, S. M., Pechatnikova, E., Wilson-Kubalek, E. M., Whittaker, M., Pate, E., Cooke, R., Taylor, E. W., Milligan, R. A., and Vale, R. D. (1999) *Nature* **402,** 778–783
16. Menz, R. I., Walker, J. E., and Leslie, A. G. W. (2001) *Cell* **106,** 331–341
17. Weber, J., Wilke-Mounts, S., Lee, R. S.-F., Grell, E., and Senior, A. E. (1993) *J. Biol. Chem.* **268,** 20126–20133
18. Weber, J., Bowman, C., and Senior, A. E. (1996) *J. Biol. Chem.* **271,** 18711–18718
19. Weber, J., Wilke-Mounts, S., Hammond, S. T., and Senior, A. E. (1998) *Biochemistry* **37,** 12042–12050
20. Turina, P., and Capaldi, R. A. (1994) *J. Biol. Chem.* **269,** 13465–13471
21. Turina, P., and Capaldi, R. A. (1994) *Biochemistry* **33,** 14275–14280
22. Brune, M., Hunter, J. L., Corrie, J. E. T., and Webb, M. R. (1994) *Biochemistry* **33,** 8262–8271
23. Brune, M., Hunter, J. L., Howell, S. A., Martin, S. R., Hazlett, T. L., Corrie, J. E. T., and Webb, M. R. (1998) *Biochemistry* **37,** 10370–10380
24. Kunkel, T. A., Bebenek, K., and McClary, J. (1991) *J. Methods Enzymol.* **204,** 125–139
25. Matsui, T., and Yoshida, M. (1995) *Biochim. Biophys. Acta* **1231,** 139–146
26. Hisabori, T., Muneyuki, E., Odaka, M., Yokoyama, K., Mochizuki, K., and Yoshida, M. (1992) *J. Biol. Chem.* **267,** 4551–4556
27. Matsui, T., Muneyuki, E., Honda, M., Allison, W. S., Dou, C., and Yoshida, M. (1997) *J. Biol. Chem.* **272,** 8215–8221
28. Jault, J. M., Matsui, T., Jault, F. M., Kaibara, C., Muneyuki, E., Yoshida, M.,

Kagawa, Y., and Allison, W. S. (1995) *Biochemistry* **34,** 16412–16418
29. Kuzmic, P. (1996) *Anal. Biochem.* **237,** 260–273
30. Ren, H., Dou, C., Stelzer, M., and Allison, S. W. (1999) *J. Biol. Chem.* **274,** 31366–31372
31. Yoshida, M., Sone, N., Hirata, H., and Kagawa, Y. (1977) *J. Biol. Chem.* **252,** 3480–3485
32. Odaka, M., Kaibara, C., Amano, T., Matsui, T., Muneyuki, E., Ogasahara, K., Yutani, K., and Yoshida, M. (1994) *J. Biochem.* (*Tokyo*) **115,** 789–796
33. Grubmeyer, C., Cross, R. L., and Penefsky, H. S. (1982) *J. Biol. Chem.* **257,** 12092–12100
34. Milgrom, Y. M., and Cross, R. L. (1997) *J. Biol. Chem.* **272,** 32211–32214
35. Milgrom, Y. M., Murataliev, M. B., and Boyer, P. D. (1998) *Biochem. J.* **330,** 1037–1043
36. Lambright, D. G., Sondek, J., Bohm, A., Skiba, N. P., Hamm, H. E., and Sigler, P. B. (1996) *Nature* **379,** 311–319
37. Rayment, I., Rypniewski, W. R., Schmidt-Base, K., Smith, R., Tomchick, D. R., Benning, M. M., Winkelmann, D. A., Wesenberg, G., and Holden, H. M. (1993) *Nature* **261,** 50–58
38. Fisher, A. J., Smith, C. A., Thoden, J. B., Smith, R., Sutoh, K., Holden, H. M., and Rayment, I. (1995) *Biochemistry*, **34,** 8960–8972
39. Smith, C. A., and Rayment, I. (1996) *Biochemistry* **35,** 5404–5417
40. Dominguez, R., Freyzon, Y., Trybus, K. M., and Cohen, C. (1998) *Cell*, **94,** 559–571
41. Vale, R. D., Milligan, R. A. (2000) *Science* **288,** 88–95
42. Sasaki, N., Shimada, T., and Sutoh, K. (1998) *J. Biol. Chem.* **273,** 20334–20340
43. Hirono-Hara, Y., Noji, H., Nishiura, M., Muneyuki, E., Hara, K. Y., Yasuda, R., Kinosita, K., Jr., and Yoshida, M. (2001) *Proc. Natl. Acad. Sci. U. S. A.* **98,** 13649–13654